

Spatial Measurement of Bed Load Transport in Tigris River

**Ammar A. Ali ¹, Nadhir A. Al-Ansari², Qusay Al-Suhail ³
and Sven Knutsson²**

Abstract

Using Helley-Smith sampler, 288 bed load samples were collected from 16 cross sections along 18 km reach length of Tigris River within Baghdad. The spatial distribution of sampling along the reach took into consideration the variance of river topography where 7 meanders, 2 islands and several bank depositions characterize the geometry of the river. The implemented regulation schemes on Tigris River have reduced 44% of water discharges compared to previous period. The spatial variance in topography was effectively scattering the results of the applied twenty bed load formulas. The study results indicated that the complicated geometry of the river reach makes finding a unique representative bed load formula along the study reach rather difficult, and there is no grantee to have good agreement with measurements in the irregular cross sections (meanders, sand bars, etc.). The closest bed load prediction formulas were van Rijn1984. The annual transported quantities of bed load were estimated to be 30 thousand tons (minimum) in 2009 and 50 thousand tons (maximum) in 2013.

Keywords: Bed load sampling, spatial bed load, Helley-Smith sampler, meandering river, sand bed, prediction formula, Tigris River.

¹ Water Resources, College of Engineering, University of Baghdad, Iraq

² Department of Civil, Environmental and Natural Resources Engineering, Lulea University of Technology, Sweden.

³ Earth Sciences, College of Science, University of Baghdad, Iraq

1 Introduction

Natural rivers transport sediment in two modes, suspended load and bed load. The former is finer and it is transported in suspension whether its source is wash load or bed sediment. While the latter “bed load” is coarser fraction and it moves in contact with the river’s bed by sliding, rolling and saltating according to the boundary shear stress. An exchange occurs between suspended and bed loads, and between bed load and bed material depending on the sizes of sediment particles, transport capacity, flow velocity, and boundary shear stress [1,2].

The main sources of fluvial sediments are watershed erosion, stream erosion and human activities [3]. Since sediment sources are unlimited and streams have sufficient sediment transport capacity, sediment transport will continue [4]. Limited Supply condition of the fine sediment is the case in most natural rivers. When the river transport capacity reduces, certain range of sediment sizes becomes heavy to be kept transported even as bed load, then the river becomes competence-limited case [1]. River bed material is the source of one of the sediment load components which is called bed-sediment load. This load’s component is transported as bed load or even in suspension and it should be distinct from the wash load as sediment source [1,2].

Prediction of bed load is of primary importance for river engineering and geomorphology [5]. Its effect on developing the bed forms, driving fluvial incision and knick point propagation [6].

It is difficult to measure bed load directly because the measuring sampler performance is affected by several parameters such as hydraulic efficiency, sampler orientation, bed-forms, bed material and so on [1,7]. However, a lot of measurements were conducted in labs and natural streams [8,9,10,11] using different samplers, such as manually operated portable samplers, vortex tube, pit and trough [12].

In this work, an attempt has been made to calculate the bed load transport rate of the northern part of Tigris River within Baghdad directly using field measurement and establish bed load rating curve using new proposed procedure for geometrical complicated river and to predict sediment bed load indirectly using mathematical formulas.

2 Tigris River

Tigris River bisects Baghdad City, the capital of Iraq, in two parts (Fig. 1) for a distance of 50 km within urban zone and 10 km within rural zones [13,14,15]. The northern part of Tigris River reach, which is considered in this work, of 18 km length extends from Al-Muthana Bridge to the north to Sarai Baghdad gauging station at the center of Baghdad (Fig. 1.B). This river reach has single thread, compound meanders, and alluvial plain characteristics. The river banks are protected against erosion by aligned stones and cement mortar between levels 29

and 37 m.a.s.l. Recently, the dominant water levels in the reach are below the protection levels [13,14,15].

During the last two decades many new islands, side depositions and point bars appeared in the Tigris River's reach within Baghdad (Fig. 1.B). These sedimentations in the river course has its impact on the hydraulic performance of the river, such as reducing its flood capacity, impeding navigation and reducing the efficiency of water intakes of water treatment plants, as well as the environmental and aesthetic impacts [14,15].

Previous study about sediment transport and river training [16] which was conducted on the river reach in Baghdad, mentioned Tigris River sediment is "bed-load". Since it found the suspended load concentrations never reach 3 g l⁻¹ in high water and never exceed 0.2 g l⁻¹ in low water periods. This study was not based on real field measurements for the bed load. Bed material samples and suspended load samples were collected only in that study. Therefore, it is important to measure the bed load discharge in Baghdad since no measurements were previously performed.

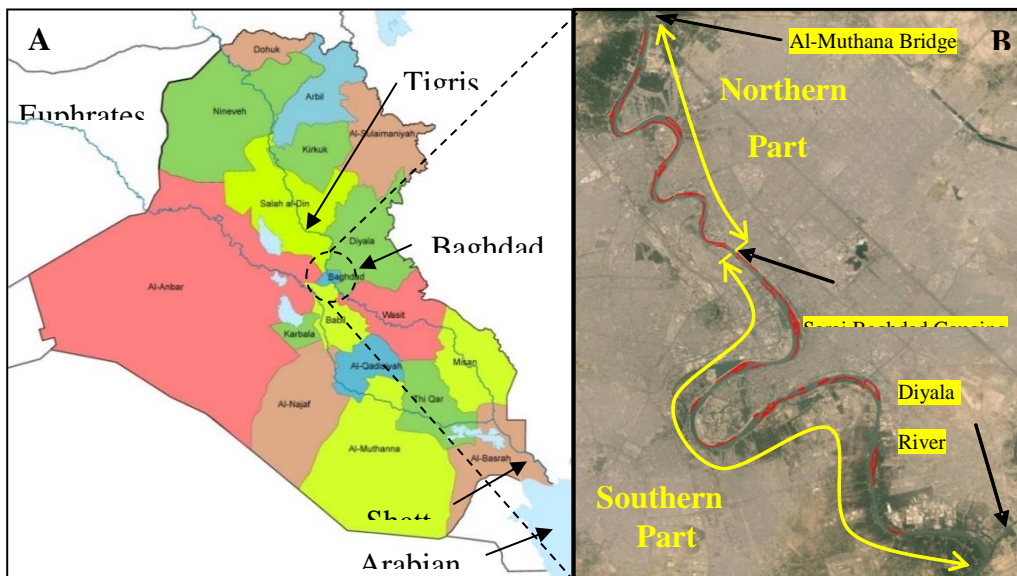


Figure 1: (A) Map of Iraqi Provinces (B) Tigris River inside Baghdad, capital of Iraq (islands and sandbars bordered by red) ([14,15])

2.1 Hydrology of Tigris River in Iraq

The flow of the river is fully controlled in Baghdad by a system of dams and regulators constructed on the main river and the tributaries upstream of Baghdad (Fig. 2) [17,18]. These regulating schemes have decreased the average monthly discharge of the river 44% according to the records of the Sarai Baghdad gauging station, it has been 522 m³s⁻¹. The Tigris River hydrograph at Sarai Baghdad (Fig.

3) shows the main delivery events of sediment into Baghdad have been vanished.

Sediment transport rates are affected in the course of Tigris River upstream of Baghdad due to the trapping of sediment within the reservoirs of the headwater.

The only uncontrolled source of sediment that can be delivered to Baghdad is the area restricted from the lower sub-basin of the Adhaim tributary and the catchment between the Samarra Barrage and Baghdad (Fig. 2), as well as the bed and banks erosions.

The delivery of fine sediment from the Adhaim Tributary has not been measured, but a glance at the possible extra flow contribution (rather than flow released from the Adhaim Dam), can give an indication for the estimated sediment delivery. The extra water flow contribution from the Adhaim Tributary sub-basin and Tharthar Lake back feed toward the Tigris River was determined using the mass balance concept. The contribution did not exceed 260 m³s⁻¹ during 2004-2005, which was a moderate year compared with recent more dry years as shown in figure (4). As an average, the extra contribution was 8% of the average monthly discharge at the Sarai Baghdad for the same year.

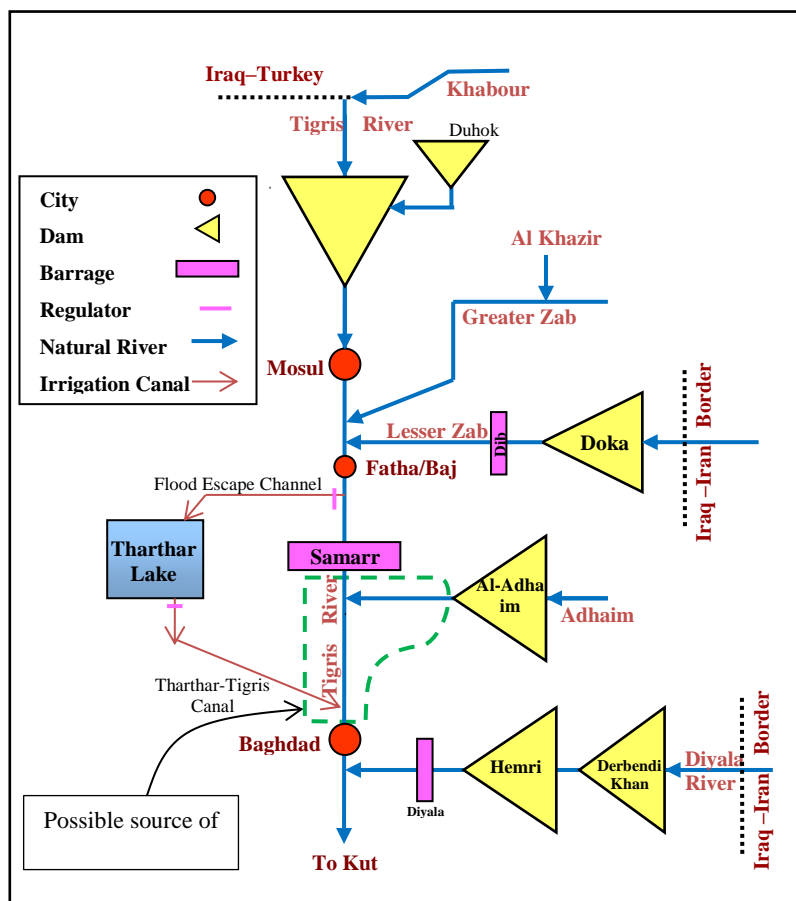


Figure 2: Schematic Diagram of Tigris River Hydrological Scheme ([19].

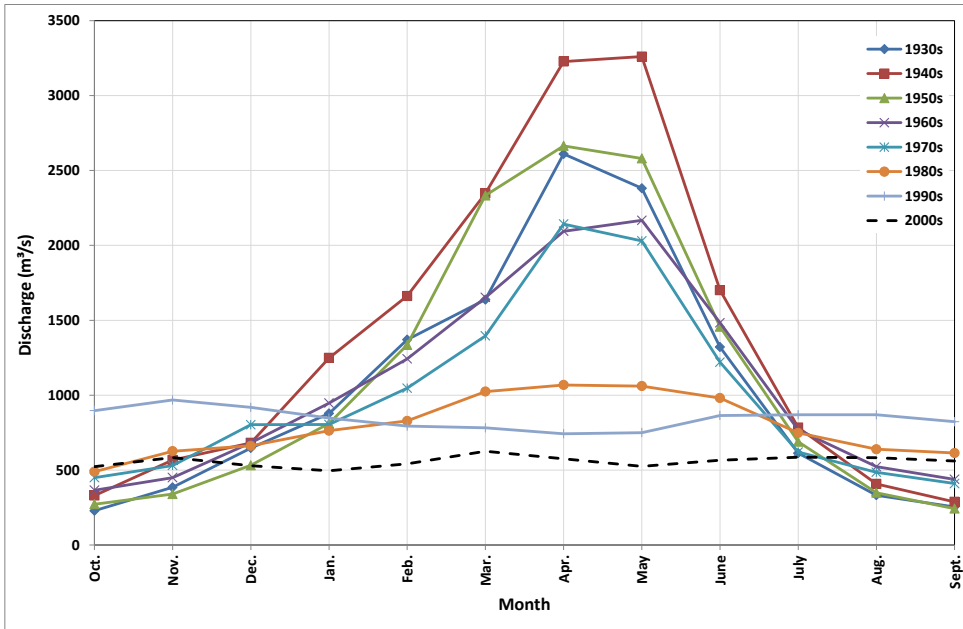


Figure 3: Hydrographs of Tigris River at Sarai Baghdad for the period 1930-2013 (data source: [20]).

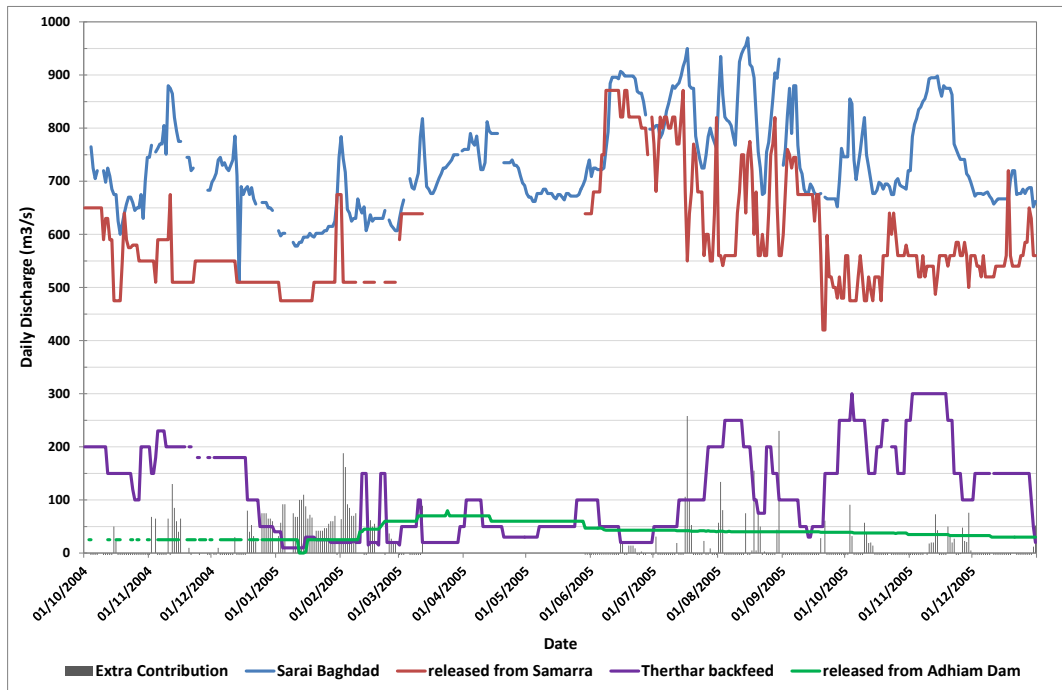


Figure 4: Contribution of runoff of Adhaim River sub-basin downstream Adhaim Dam to Tigris River discharges for the year 2004~2005.

2.2. River Geometry and Bed Composite

The morphology and the bed sediment of the river were investigated several times inside Baghdad by [16,21,22,23,24]. Rapid changes in the bed material from gravel in Samarra to fine sand in Baled (50 km to the downstream of the Samarra Barrage and 130 km to the upstream of Baghdad) [25] The riverbed was already sand bed between Baled and Baghdad even before the construction of the Samarra Barrage in 1956.

The geometry of the study area consists of a series of 7 meanders (Fig. 5) of radii of curvature are ranging from 475m to 1245m [23]. Along the second meander (CS4, CS4-2 and CS5) an island is noticed directly upstream of CS4 and the river cross section transfers from riffle at CS4 to pool at CS4-2 and CS5 and the higher velocity zone is also transferred from the inner bank of CS4 to the center of CS4-2 then to the outer bank of CS5. This change in the velocity field gives an indication about the attempts of the river to shift the peak of the meander to the downstream of its' current location. This can explain the high depositions on the outer bank between CS4 and CS4-2.

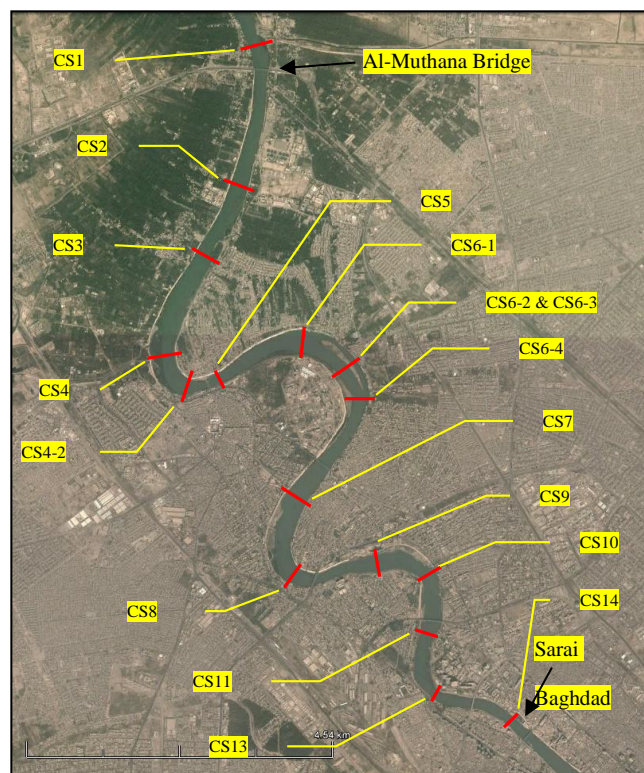


Figure 5: Bed load sampling cross sections along the northern part of Tigris River ([14,15])

The same velocities distribution is repeated at the 4th and 5th meanders (CS8 and CS10 respectively), where the higher velocities are in the centers of the sections and large depositions existed in the front halves of the concave banks. At the third meander (CS6-1, CS6-2, CS6-3 and CS6-4), a large island mediates the meander. The sections CS6-1 and CS6-4 are of pool type while the sections CS6-2 and CS6-3 are of run type. Depositions are existed along the inner bank of the meander. Mean velocities in both branches are equal while the top width of the right branch is 2.2 times the left branch. Using the van Veen grab, 46 bed-material samples were collected along the northern reach in Baghdad. The particle size distribution was analysed using the sieves and the hydrometer. It was noticed that fine sand dominant the riverbed. The average median size was 0.178 mm [26]. The size of the bed sediment relatively decreased compared to earlier investigations (see [21] Al-Ansari and Toma 1984). In addition, the sediments were moderately sorted, fine skewed and leptokurtic ([26].

3. Bedload Sampling

A Helley-Smith sampler was manufactured of 3" × 3" (76 mm × 76 mm) opening size and 3.5 exit/entrance expansion ratio. Other dimensions of the sampler were taken from van Rijn (2007). Two exceptions were considered, the weight of the sampler and the size of the mesh bag. The original weight of the sampler was reduced to 15kg, which makes it easier handling in small boat without winch. No problem in the performance was expected to be due to the reduced weight since the average velocity in the river did not reach 1 m s⁻¹. Furthermore, avoiding the oversampling that may occur due to the scooping effect [9,10] is more valuable. Larger mesh bag of 2200 cm² surface area was used to maintain the sampling efficiency in case the bag is filled for more than 40% of volume and to avoid clogging the bag openings by close size particles and organic materials [27, 28,29]. At the quartiles of 16 cross sections (Fig. 5), 288 bed load samples were collected. Sampling times were 60s of 238 samples, 120s of 2 samples, and 300 s of a single sample. The separation period was 3 min between 5 sequences samples at each sampling point to determine the time-averaged rate of sediment transport. Zero-time samples were collected at the sampling points to overcome the initial and scooping effect of the sampler on the bed [29]. Velocity profile measurements were conjugated with bed load sampling in all cross sections using SonTek River Surveyor ADCP. The mean weight was determined for the repetitions of the same sampling point. The weights of zero-time samples were subtracted from the means. A reduction factor of 0.5 was applied to the modified means considering the trapping efficiency as 200% for fine sand. Table (1) shows the measured bed load discharge for each cross section along the reach with the bed sediment properties and the hydraulic-geometric parameters those are associated or existed during measurements.

The maximum bed load transport rate was 3.938 kg s⁻¹ at CS8 associated with

a water discharge of 643.5 m³s⁻¹ and the minimum was 0.6822 kg s⁻¹ at CS4 associated with a water discharge of 449 m³s⁻¹. The average bed load transport rate was 2.099 kg s⁻¹ with 0.889 standard deviation.

The scattering in some of bed load measurements can be attributed to the spatial variation in river topography along the study reach where it is an influencing factor, as well as, bed sediment size, particle size distribution and bed shear stresses [30] in case there is no external source of disturbance.

4. Spatial Distribution of Bed load

The variance in the topography and morphology in the Tigris River was reflected in the spatial distribution of bed load and velocity field as shown in figure (6). This figure shows the distribution of the measured bed load discharges per unit width at sampling points along the study reach as well as bed shear stresses. The data series are not in the sequence of display in the figure and separation lines were used to specify cutting in the data series and also to specify the relative parts of each data series to a certain cross section. The following description for the spatial distribution of bed load was associated with the measured velocity distribution using ADCP at the sampling time.

Table 1: The measured bed load rates with the bed sediment properties and hydraulic-geometric parameters along the northern reach of Tigris River

C.S.	d_{50} (mm)	d_{90} (mm)	Cross-sectiona l Area (m ²)	Top Width (m)	Hydraulic Radius (m)	Discharge (m ³ s ⁻¹)	Water velocity (ms ⁻¹)	Bedload rate (kgs ⁻¹)
CS1	0.194	0.273	664.9	180.03	2.98	457.381	0.688	1.268
CS2	0.166	0.235	653.7	260.77	2.471	459.022	0.702	2.590
CS3	0.1755	0.25	795.2	261.6	3.008	464.409	0.584	1.341
CS4	0.199	0.273	691.5	250.06	2.743	445.095	0.644	0.682
CS4-2	0.197	0.276	745	241.09	3.013	452.325	0.607	1.142
CS5	0.208	0.278	643.3	151.67	4.072	489.233	0.76	1.599
CS6-1	0.199	0.273	865.2	353.85	2.398	549.877	0.636	2.901
CS6-2	0.21	0.275	421.284	185.2	2.271	286.409	0.68	0.924
CS6-3	0.145	0.255	369.83	83.37	4.113	251.023	0.679	0.190
CS6-4	0.19	0.27	760.4	237.8	3.141	561.778	0.739	3.420
CS7	0.2	0.277	932.7	320.08	2.881	651.709	0.699	1.564
CS8	0.2	0.275	979	236.86	4.053	643.319	0.657	3.938
CS9	0.12	0.218	772.9	255.5	2.911	530.443	0.686	2.171
CS11	0.143	0.243	1128.40	213.99	5.279	578.375	0.513	2.716
CS13	0.197	0.276	720.6	114.9	5.889	529.965	0.735	2.630
CS14	0.135	0.213	711.4	137.84	4.976	522.226	0.734	2.579

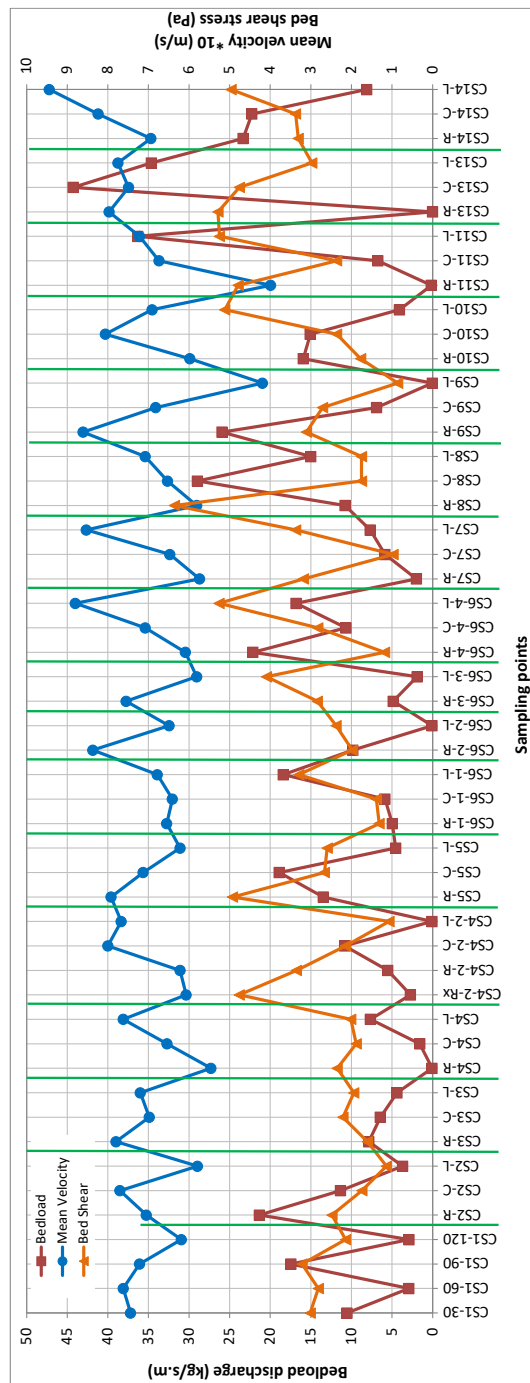


Figure 6: The measurements of the bed load discharges with the measured velocity and the calculated bed shear stresses at the sampling points along the Tigris River study reach.

CS1: The section is a run section type. Some stagnation was on the extreme left side because it is located in the shade of bank deposition. Bed load was oscillating across the section. Velocity was uniform except on the extreme left side

CS2: Bank deposition was growing on the left side where flow velocity was low. Bed load was higher towards the right.

CS3: The section is located directly downstream of a large bank deposition. Its left side is hidden by the deposition and the velocity was higher on the right side. The bed load was low in the section; however, it was little higher on the right side.

CS4: The section is located between a small island to the upstream and an acute meander to the downstream. The right side was stagnant because it is hidden behind the island and the velocity increased towards the left side. The bed load was higher towards the left side. Eddies were noticed on the right side.

CS4-2: The section is pool type, deeper on the right side. It's located at the center of an acute meander. On the deeper side, velocity was not at its highest, higher velocities were closer to the center. The bed load was higher in the center.

CS5: The section is pool type, deeper on the right side. Velocity and bed shear were higher on the right side. However, the bed load was higher in the center of the section due to the effect of the secondary flow, since the section is within the downstream half of an acute meander.

CS6-1: The section is pool type; deeper on the left side. The velocity distributed uniformly across the section. The bed load was higher on the left side.

CS6-2: The section is the inner branch of a meander that is bisected by an island. The left side of the section was a trench produced by excavators, so the velocity was low by comparison with the right side. The bed load was higher on the right side where the velocity was higher.

CS6-3: The section is the outer branch of the meander. The flow was turbulent on the most outer side. Bed load was low at all.

CS6-4: The center of the section was close to the tail of a large island, so the secondary flow at the confluence of the two branches was the reason behind the high bed load on both sides.

CS7: The section is of a riffle type. The velocity on the left side was higher, while on the right side, although the bed shear was relatively high, the bed load was low because the velocity was also low.

CS8: The section is pool type; deeper on the right side. However, the velocity was neither high nor was the bed load. The highest bed load was in the center due to the effect of the secondary flow.

CS9: The main flow was on the right side while the left side was stagnant, so bed load was higher on the right and lower on the left.

CS10: The section is pool type, deeper on the left side. The bed load was lower due to higher bed shear, which may suspend the bed sediment.

CS11: The section is the riffle type. Although the right side has the same depth as the left, but bed load was much higher on the left because the right side was stagnant and recently dredged.

CS13: The section is pool type, deeper on the right. The bed load was lower on the right due to higher bed shear, which may suspend the bed sediment. The bed load was higher in the center due to the effect of secondary flow.

CS14: The section is pool type, deeper on the left. The bed load was lower on the left due to higher bed shear and higher flow velocity, suspend the bed sediment.

5. Bed load Prediction Using Formulas

Wide spectrums of bed load predicting formulas were proposed and developed by many researchers depending on different approaches. For each approach, a specified concept was considered as motivation for deriving the approach's formula and a certain number of parameters were controlled in the lab measurements to estimate the formula parameters.

5.2. Approaches of Bed load Formulas

Twenty bed load formulas were selected and applied on the study reach to predict the bed load discharge to find the best suitable formulas. Brief descriptions for the used approaches are given below:

5.2.1. Shear stress approach

The movement of bed material particles will start when the criteria of incipient motion is exceeded. So, shear stress near the bed will entrain the sediment particles to motion as long as the shear stress is greater than the critical shear stress of the particles. The following formulas which belong to this approach were used in this work:

- a. DuBoys₁₉₃₅ formula [31]
- b. Shields₁₉₃₆ formula [32]
- c. Kalinske₁₉₄₇ formula [32]
- d. Cheng-Simons-Richardson₁₉₆₅ formula [32]
- e. Wong-Parker₂₀₀₆ formula [33]

5.2.2. Energy slope approach

The bed load motion is initiated due to the portion of energy losses coming from the grain resistance [32]. The following formulas were used from this approach:

- a. Meyer-Peter₁₉₃₄ formula [3]
- b. Meyer-Peter-Muller₁₉₄₈ formula [31]

5.2.3. Discharge approach

In natural rivers, critical unit discharge was used as an indication on starting bed load sediment motion when it is exceeded by water discharge [34]. The following formulas which belong to this approach were used in this work:

- a. Schoklisch_{1934, 1943} Formula [32]
- b. Casey₁₉₃₅ formula [22]

Probabilistic approach

Probability concepts were introduced in bed load prediction by the pioneer work of Einstein in 1942 [31]. The turbulent flow fluctuations are the driver for sediment entrainment rather than the flow forces exerted on the particle. Both of the entrainment and the deposition were expressed in probability terms [32].

- a. Einstein₁₉₅₀ bed load function [31]
- b. Einstein-Brown₁₉₅₀ formula [31]

5.2.4. Regression approach

Data driven models (regression, ANN) were used to explain the bed load transport process due to the limitations of defining this complex process into precise formula [34]. The following formulas were used within this approach:

- a. Rottner₁₉₅₉ formula
- b. Yalin₁₉₆₃ formula [35]
- c. Van Rijn₁₉₈₄ formula [36]
- d. Julien₂₀₀₂ formula [37]
- e. Camenen-Larson₂₀₀₅ formula [38]

5.2.5. Equal mobility approach

The flow forces act on the exposed particles causing mobilization with possibility of participation of the substrate particles into bed load movement at scour zones due to their exposure on the surface [32].

- a. Wilcock₂₀₀₁ formula [39]
- b. Wilcock-Crowe₂₀₀₃ formula [40]

5.2.6. Power Concept

This approach has developed from the concept that there is a relation between the available energy to the river with the rate of work done by the river to transport sediment [32]. The following formula was used within this approach:

- a. Bagnold₁₉₆₆ formula

5.3. Application of Bedload Formulas

Two kinds of datasets were required for applying bedload formulas, physical properties of river bed sediment and hydraulic-geometric parameters of the study reach. Sediment characteristics were determined from the size analysis of the bed materials samples. The hydraulic-geometric parameters included; water depth, cross sectional area, top width, wetted perimeter, hydraulic radius, water surface slope and water discharge. These datasets were extracted from field measurements in the sampled cross sections. The results published by [26] contained most of the datasets, whilst other datasets were listed in table 1.

The results of the bed load formulas at sixteen cross sections along the study reach were compared with the measured bed load discharges in the same section and two indicators were used to measure the accuracy of the predicted bed load. The discrepancy ratio, which is the ratio of predicted bed load to measured one [36], was one of the indicators and the error percentage [41] was the other. The comparisons of results are shown in figure (7). Six zones of different discrepancy ratios were specified in the figure to explain the distribution of the results around the perfect agreement line.

Most of the formulas overestimated the bed load transport rate by more than 10 times and even 100 times relative to field measurements. Five formulas from four of the approaches predicted bed load discharges close to measurements. These formulas were Meyer-Peter1934, Schoklitsch1934, 1943, van Rijn1984 and Einstein1950 bed load function with average discrepancy ratios of 0.5, 1.51, 0.47, 1.18 and 4.06 respectively. The predictions of van Rijn1984 and Schoklitsch1934 formulas are distributed on both sides of the perfect agreement line. Whilst both of Meyer-Peter1934 and Schoklitsch1943 formulas are mainly bounded between the perfect line and discrepancy ratio $\frac{1}{4}$. Some results of Einstein1950 were in the area between the perfect agreement and $r = 8$.

Table (2) shows the accumulated percentages of the predicted bed load discharges according to each range of the discrepancy ratio. The higher percentage of predicted bed load within the closer range of discrepancy ratio 0.75 ~ 1.25 (Error% = -25 ~ +25) was equally between Schoklitsch1934 and van Rijn1984 formulas and the results approximately continued in this manner until the third zone of discrepancy $\frac{1}{2} \sim 2$ (Error% = -50 ~ +100). At this range, more than 76% of Schoklitsch1934 and 53% and of van Rijn1984 predictions were located within the range. The percentages of the other three formulas didn't exceed 24% for the discrepancy range $\frac{1}{2} \sim 2$ (Error% = -50 ~ +100).

To clarify the behaviour of the bed load formulas at different cross sections, having varied morphological characteristics, the formulas were applied for a range of discharges between 400 and 700 m^3s^{-1} at some sections along the reach.

Figure (8) show that Einstein's formula was over-predicting in all sections and it showed multiple points of change in the slope at cross sections CS1, CS6-1, CS7 and CS9 depending on the water flow, whilst at sections CS6-4, CS11 and CS14, the formula curves were smoother. The Meyer-Peter1934 and Schoklitsch1943

formulas were always under-predicting. The Schoklitsch1934 and van Rijn formulas fluctuated between the measurements being under and over depending on the characteristics of the cross section.

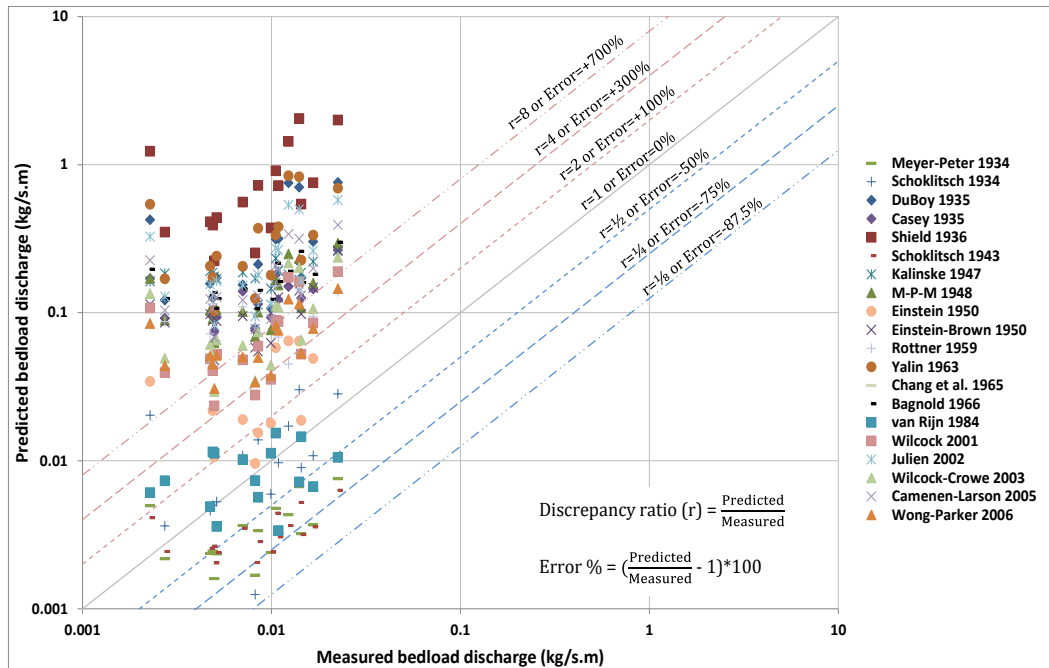


Figure 7: Comparison of bed load discharges predicted by different bed load formulas with measured bed load in Tigris River.

It is not clear that there is a unique prediction formula that can predict the bed load discharge with stable magnitude of error along the whole study reach. The important conclusion from the application results is, even for those formulas have agreement with field measurements in regular cross sections, there is no guarantee to have the same agreement in the irregular cross sections (meanders, sand bars, etc.). Annual bed load quantities were computed using all the formulas for the period 2009-2013 along the study reach and are listed in table 3. The annual bed load quantities are ranging from 36 thousand ton (minimum) in 2009 to 50 thousand ton (maximum) in 2013 according to van Rijn1984 formula.

6. Conclusions

The implemented regulation scheme on the Tigris River has limited the sources of sediment supply; it has also decreased the average water flow to 44% compared to previous periods. The spatial distribution of the bed load was effected by the bed shear and the flow velocity at the sampling point. Whenever the velocity and

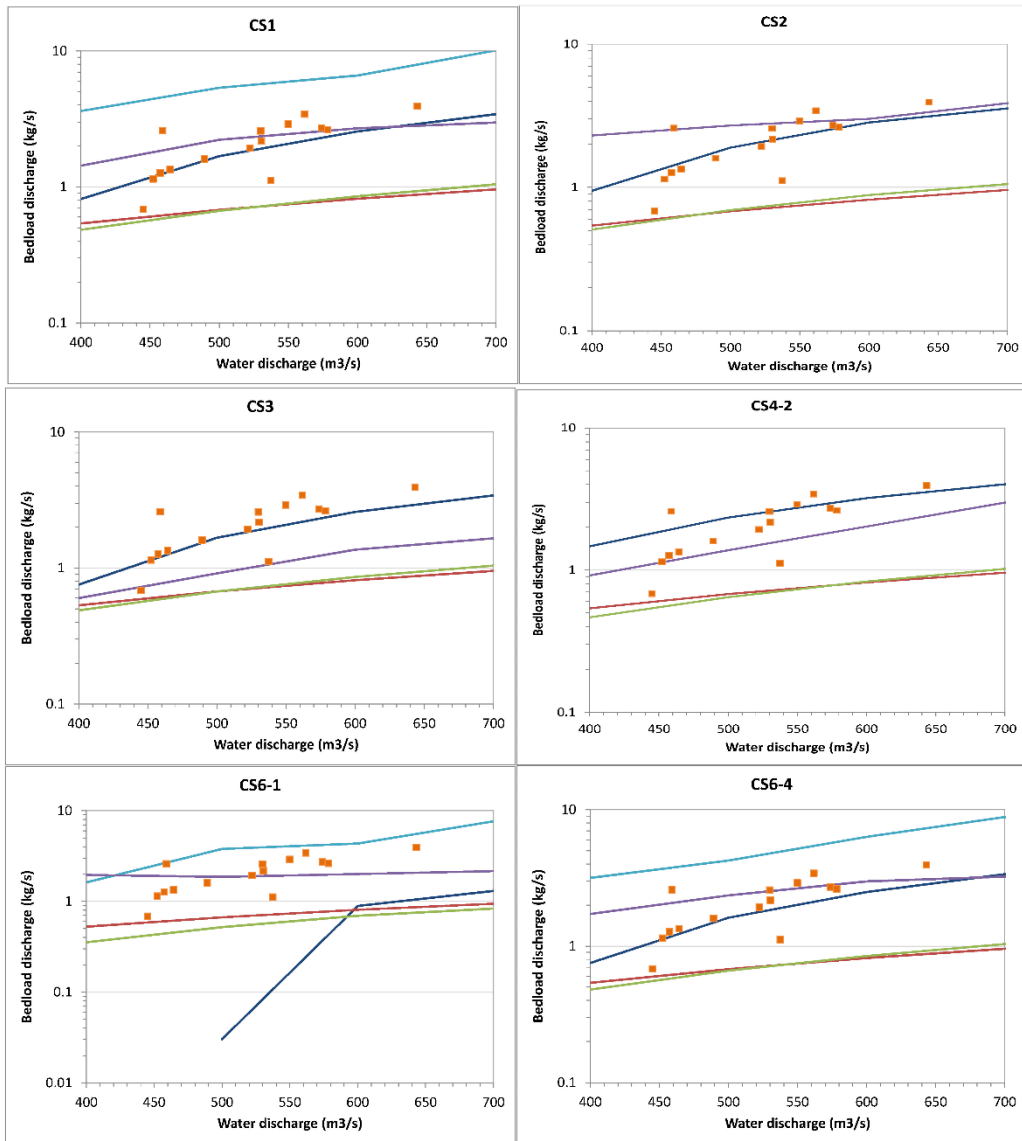
the bed shear increase, the bed load increases also for certain limit depending on the particle size then it may transfer to suspension. Some exceptions are expected in the meanders due to the secondary current, where the bed load increases for a lower velocity and/or bed shear. The complicated geometry of the river reach makes finding a unique representative bed load formula along the study reach rather difficult. Furthermore, even for those formulas having agreement with field measurements in regular cross sections, there is no guarantee to have the same agreement in the irregular cross sections (meanders, sand bars, etc.). The closest bed load prediction formulas were van Rijn 1984 then Schoklitsch 1934 and the average discrepancy ratios were of the order 1.18 and 1.51 respectively. Annual bed load quantities were estimated for the period 2009-2013 to be 36 thousand tons (minimum) in 2009 and ranged to 50 thousand tons (maximum) in 2013 according to the van Rijn 1984 formula. The average annual transport rate for the period 2009-13 was 42.6 thousand tons.

Table 2: Accumulative percentages of predicted bed load according to the ranges of discrepancy ratio.

Formulas	Ranges of discrepancy ratio and corresponding error percentages				
	0.75 ~ 1.25	0.67 ~ 1.5	½ ~ 2	¼ ~ 4	⅛ ~ 8
	-25 ~ +25	-33 ~ +50	-50 ~ +100	-75 ~ +300	-87.5 ~ +700
Meyer-Peter ¹⁹³⁴	5.88	5.88	17.65	76.47	100
Schoklitsch ¹⁹³⁴	23.53	47.06	76.47	82.35	88.24
DuBoy ¹⁹³⁵	0	0	0	0	0
Casey ¹⁹³⁵	0	0	0	0	0
Shield ¹⁹³⁶	0	0	0	0	0
Schoklitsch ¹⁹⁴³	5.88	5.88	23.53	82.35	100
Kalinske ¹⁹⁴⁷	0	0	0	0	0
M-P-M ¹⁹⁴⁸	0	0	0	0	11.76
Einstein ¹⁹⁵⁰	5.88	11.76	23.53	41.18	64.71
Enistein-Brown ¹⁹⁵⁰	0	0	0	0	23.53
Rottner ¹⁹⁵⁹	0	0	0	5.88	23.53
Yalin ¹⁹⁶³	0	0	0	0	0
Chang et al. ¹⁹⁶⁵	0	0	0	23.53	70.59
Bagnold ¹⁹⁶⁶	0	0	0	0	0
van Rijn ¹⁹⁸⁴	23.53	41.18	52.94	94.12	94.12
Wilcock ²⁰⁰¹	0	0	0	17.65	47.06
Julien ²⁰⁰²	0	0	0	0	0
Wilcock-Crowe ²⁰⁰³	0	0	0	0	29.41
Camenen-Larson ²⁰⁰⁵	0	0	0	0	0
Wong-Parker ²⁰⁰⁶	0	0	0	11.76	58.82

Table 3 Annual bed load predicted discharges for the period 2009~2013.

Year	2009	2010	2011	2012	2013	Average
Meyer-Peter ¹⁹³⁴	17.88	21.07	19.59	21.96	24.61	21.02
Schoklitsch ¹⁹³⁴	50.51	64.89	57.52	68.51	81.87	64.66
DuBoy ¹⁹³⁵	1727.07	2009.06	1880.12	2087.37	2318.04	2004.33
Casey ¹⁹³⁵	680.44	787.01	739.41	818.28	902.62	785.55
Shield ¹⁹³⁶	4085.10	4919.11	4512.47	5125.81	5885.69	4905.63
Schoklitsch ¹⁹⁴³	17.52	20.01	18.93	20.75	22.66	19.97
Kalinske ¹⁹⁴⁷	1116.36	1187.90	1170.03	1215.75	1246.16	1187.24
M-P-M ¹⁹⁴⁸	809.65	908.84	868.22	939.89	1010.68	907.46
Einstein ¹⁹⁵⁰	163.65	178.58	173.43	183.72	193.62	178.60
Enistein-Brown ¹⁹⁵⁰	572.10	649.50	616.26	672.13	728.98	647.79
Rottner ¹⁹⁵⁹	548.02	635.31	595.40	657.92	735.67	634.46
Yalin ¹⁹⁶³	2330.52	2636.03	2507.32	2729.70	2955.13	2631.74
Chang et al. ¹⁹⁶⁵	282.77	337.27	309.33	344.63	409.49	336.70
Bagnold ¹⁹⁶⁶	897.41	1019.74	967.51	1056.16	1147.13	1017.59
van Rijn ¹⁹⁸⁴	36.17	42.58	39.56	44.23	50.50	42.61
Wilcock ²⁰⁰¹	461.07	527.38	498.35	546.79	598.19	526.36
Julien ²⁰⁰²	1441.44	1644.19	1555.99	1703.37	1860.09	1641.02
Wilcock-Crowe ²⁰⁰³	576.33	659.22	622.94	683.49	747.74	657.95
Camenen-Larson ²⁰⁰⁵	1024.46	1158.42	1102.02	1199.45	1298.11	1156.49
Wong-Parker ²⁰⁰⁶	399.76	448.85	428.72	464.20	499.27	448.16



— Schoklitsch 1934 — Schoklitsch 1943 — Meyer-Peter 1934
— Einstein 1950 — van Rijn 1984 ■ Measurements

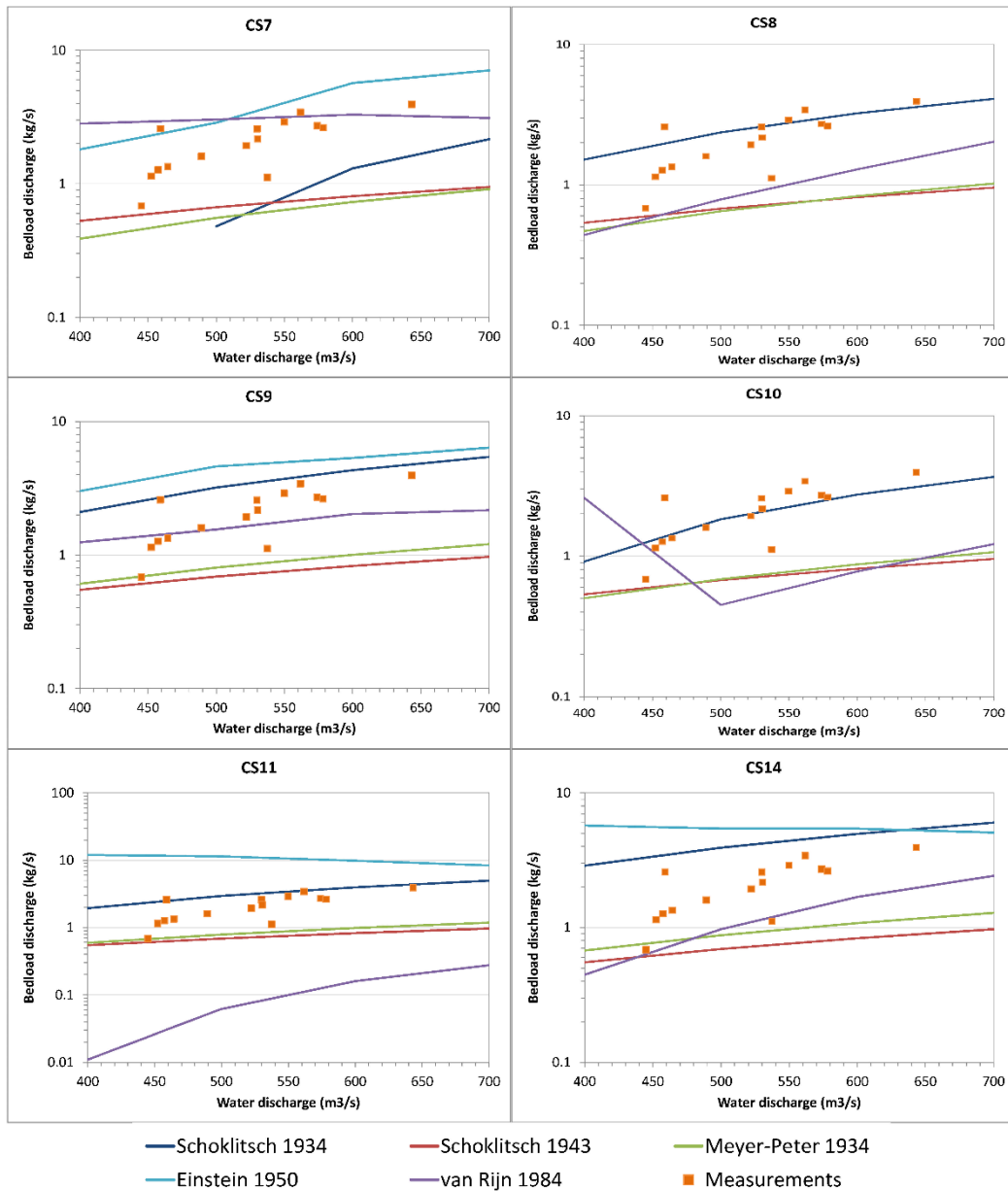


Fig. 8 Application of bedload formulas and rating curve at different cross sections for a range of discharges.

References

- [1] Hickin, E.J., 1995. River Geomorphology. Wiley.

- [2] World Meteorological Organization (WMO), 2003. MANUAL ON SEDIMENT MANAGEMENT AND MEASUREMENT. OPERATIONAL HYDROLOGY REPORT No. 47, WMO-No. 948.
- [3] Vanoni, V.A., 2006. Sedimentation Engineering. ASCE manuals and reports on engineering practice No. 54. Virginia: ASCE.
- [4] Friend, P.F., 1993. Control of river morphology by the grain-size of sediment supplied. *Sediment. Geol.*, 85, 171-177.
- [5] Recking, A., 2009. Theoretical development on the effects of changing flow hydraulics on incipient bed load motion. *WATER RESOURCES RESEARCH*, 45 (W04401).
- [6] Cook, K.L., Turowski, J.M, and Hovius, N., 2013. A demonstration of the importance of bedload transport for fluvial bedrock erosion and knickpoint propagation. *Earth Surf. Process. Landforms*, 38, 683–695.
- [7] Gaudet, J.M., Roy, A.G. and Best, J.L., 1994. EFFECT OF ORIENTATION AND SIZE OF HELLEY-SMITH SAMPLER ON ITS EFFICIENCY. *J. Hydraul. Eng.*, 120, 758-766.
- [8] Helley, E.J. and Smith, W., 1971. DEVELOPMENT AND CALIBRATION OF A PRESSURE-DIFFERENCE BEDLOAD SAMPLER. OPEN-FILE REPORT, USGS, California.
- [9] Gaweesh, M.T.K. and van Rijn, L.C., 1994. BED-LOAD SAMPLING IN SAND-BED RIVERS. *Journal of Hydraulic Engineering*, 120 (12), 1364-1384.
- [10] Bunte, K and Abt, S.R., 2009. Transport Relationships between Bedload Traps and a 3-Inch Helley-Smith Sampler in Coarse Gravel-Bed Streams and Development of Adjustment Functions. Completion Report No. 218. Colorado Water Institute.
- [11] Atkinson, E., 1994. Vortex-tube sediment extractors I: trapping efficiency. *J. Hyd. Engr. ASCE*, 120(10), 1110–25.
- [12] Strahlhofer, L.K., 2010. Continuous Bedload Transport Measurements and Calibration Purposes using a Hydraulic Lifiable Slot Trap. Thesis (M.Sc.). Lincoln University.
- [13] Ali, A.A., 2013. Morphology of Tigris River inside Baghdad City. Thesis (Licentiate). Lulea University of Technology.
- [14] Ali, A.A., Al-Ansari, N.A. and Knutsson, S., 2012. Morphology of Tigris River within Baghdad City. *Journal of Hydrology and Earth System Sciences*, 16, 3783-3790.
- [15] Ali, A.A., Al-Suhail, Q., Al-Ansari, N.A. and Knutsson, S., 2014. Evaluation of Dredging Operations for Tigris River within Baghdad, Iraq. *J. Water Resources and Protection*, 6 (4), 202-213.
- [16] Geohydraulique, 1977. Tigris River Training Project within Baghdad City. Report Submitted to the Iraqi Ministry of Irrigation, Paris.
- [17] Al-Ansari, N.A., 2013. Management of Water Resources in Iraq: Perspectives and Prognoses, *Engineering*, 5(8), 667-684.

- [18] Al-Ansari, N.A., 2016. Hydropolitics of the Tigris and Euphrates Basins, *Engineering*, 8(3), 140-172.
- [19] Ministry of Water Resources - Iraq (MWR), 2005. Schematic diagram of main control structures in Iraq. General directorate of water resources management, hydrological studies centre.
- [20] Al-Shahrabaly, Q.M., 2008. River discharges for Tigris and Euphrates gauging stations (in Arabic). Baghdad: Ministry of Water Resources.
- [21] Al-Ansari, N.A., and Toma, A., 1984. Bed characteristics of the River Tigris within Baghdad. *J. Water Res.*, 3(1), 1-23.
- [22] Khalaf, R.M., 1988. Modelling sediment transport load in Tigris River within Baghdad City. Thesis (M.Sc.), University of Baghdad, Iraq.
- [23] University of Technology - Baghdad, 1992. Training of Tigris River inside Baghdad City. Report Submitted to the Iraqi Ministry of Agriculture and Irrigation, Baghdad.
- [24] Al-Ansari, N.A., Ali, A., and Knutsson, S., 2015a. Iraq Water Resources Planning: Perspectives and Prognoses. ICCCE 2015: XIII International Conference on Civil and Construction Engineering. Jeddah, 26-27 January, 2097-2108.
- [25] Hardy, F.S., Lacey, G., ALLEN, F.H., WOLF, P.O., ADDISON, H., RICHARDS, B.D., STEPHENSON, H.W., DATH, F.P., and MIDDLETON, A.A., 1956. Discussion on SOME HYDRAULIC INVESTIGATIONS IN CONNEXION WITH THE WADI THARTHAR PROJECT, IRAQ. ICE proceeding: engineering divisions. 5 (4), 352-365.
- [26] Al-Ansari, N.A., Ali, A., Al-suhail, Q. and Knutsson, S., 2015b. Flow of River Tigris and its Effect on the Bed Sediment within Baghdad, Iraq. *Open Engineering*, 5, 465-477.
- [27] Druffel, L., Emmett, W.W., Schneider, V.R., and Skinner, J.V., 1976. LABORATORY HYDRAULIC CALIBRATION OF THE HELLEY-SMITH BEDLOAD SEDIMENT SAMPLER. Mississippi: DEPARTMENT OF THE INTERIOR-GEOLOGICAL SURVEY.
- [28] Beschta, R.L., 1981. Increased bag-size improves Helley-Smith bedload sampler for use in streams with high sand and organic matter transport. *Int. Assoc. of Hydro. Sci.*, a Syrup. 133, 17-25.
- [29] van Rijn, L.C., and Gaweesh, M.T.K., 1992. NEW TOTAL SEDIMENT-LOAD SAMPLER. *Journal of Hydraulic Engineering*, 118, 1686-1691.
- [30] Julien, P.Y., 2010. *Erosion and Sedimentation*. USA: Cambridge University Press.
- [31] Graf, W.H., 1971. *Hydraulics of sediment transport*. USA: McGraw-Hill.
- [32] Yang, C.T., 1996. *Sediment transport: theory and practice*. USA: McGraw-Hill.
- [33] Wong, M. and Parker, G., 2006. RE-ANALYSIS AND CORRECTION OF BEDLOAD RELATION OF MEYER-PETER AND MÜLLER USING

- THEIR OWN DATABASE. *Journal of Hydraulic Engineering*, 132 (11), 1159-1168.
- [34] Talukdar, S., Kumar, B. and DUTTA, S., 2012. PREDICTIVE CAPABILITY OF BEDLOAD EQUATIONS USING FLUME DATA. *J. Hydrol. Hydromech.*, 60 (1), 45–56.
- [35] Yalin, S.M., 1977. *Mechanics of Sediment Transport*. UK: Pergamon Press.
- [36] van Rijn, L.C., 1993. *PRINCIPLES OF SEDIMENT TRANSPORT IN RIVERS, ESTUARIES AND COASTAL SEAS*. Amsterdam: Aqua Publications.
- [37] Julien, P.Y., 2002. *River Mechanics*. USA: Cambridge University Press.
- [38] Camenen, B. and Larson, M., 2005. A general formula for non-cohesive bed load sediment transport. *Estuarine, Coastal and Shelf Science*, 63, 249–260.
- [39] Wilcock, P.R., 2001. TOWARD A PRACTICAL METHOD FOR ESTIMATING SEDIMENT-TRANSPORT RATES IN GRAVEL-BED RIVERS. *Earth Surface Processes and Landforms*, 26, 1395–1408.
- [40] Wilcock, P.R. and Crowe, J.C., 2003. Surface-based Transport Model for Mixed-Size Sediment. *Journal of Hydraulic Engineering*, 129 (2), 120-128.
- [41] Walling, D.E., 1977. Assessing the Accuracy of Suspended Sediment Rating Curves for a Small Basin. *Water Resources Research*, 13(3), 531-538.